Chapter 4
Green Synthesis of Gold Nanoparticles by Using Natural Gums

Alle Madhusudhan, Ganapuram Bhagavanth Reddy, and Indana Murali Krishana

4.1 Introduction

Nanomaterials are cornerstones of nanoscience and nanotechnology, which constitute an interdisciplinary field that uses principles of chemistry, biology, physicsand engineering to design and fabricate nanoscale materials (Farokhzad and Langer 2009; Husen and Siddiqi 2014a, b, c; Siddiqi and Husen 2016a, b, c, d, 2017a, b; Siddiqi et al. 2016, 2018a, b). It has already caused a significant commercial impact, which will surely increase in the near future. Nanoscale materials are defined as a set of substances where at least one of their dimensions is less than 100 nm. Metallic nanoparticles (NPs) are definitely among the most widely studied systems in the modern nanoscience (Mirkin 2005) due to the fact that metals often have totally different properties when brought down to the nanometer dimensions. Metal NPs are important due to their extreme small size and large surface-to-volume ratio, which make them differ in properties from their native metals (Daniel and Astruc 2004; Bogunia-Kubik and Sugisaka 2002; Zharov et al. 2005). The design and manufacture of inorganic nanomaterials with novel applications can be achieved by controlling the size and shape at nanoscale. Nanoparticles (NPs) exhibit shape- and size-dependent properties, which are suitable for various applications such as

A. Madhusudhan (✉)
Department of Chemistry, Samskruti College of Engineering & Technology, Kondapur, Hyderabad, Telangana State, India

Department of Chemistry, University College of Science, Osmania University, Hyderabad, Telangana State, India

G. B. Reddy
Department of Chemistry, Palamuru University, Mahbubnagar, Telangana State, India

I. M. Krishana
Department of Chemistry, Samskruti College of Engineering & Technology, Kondapur, Hyderabad, Telangana State, India

A. Husen, M. Iqbal (eds.), *Nanomaterials and Plant Potential*,
https://doi.org/10.1007/978-3-030-05569-1_4

antimicrobial activity, chemical sensors, catalysis, drug delivery systems, filters and medical radiographic images. Because of their biocompatibility, stability, nontoxicity and oxidation resistance, gold nanoparticles have a specific significance in biomedical applications and in the emerging interdisciplinary fields of science (Husen 2017; Siddiqi and Husen 2017a). They show distinguished surface plasmon resonance (SPR) absorption properties, which are strongly related to their size, shape and interparticle distance. Their large surface-to-volume ratio can become a basis for a large variety of catalytic applications (Corma and Serna 2006; Dimitratos et al. 2012). For example, they exhibit (a) catalytic reduction in the gas-phase selective hydrogenation of 1,3-butadiene to butane, (b) catalytic reduction of 4-nitrophenol and hexacyanoferrate (III) by sodium borohydride, and (c) the Suzuki–Miyaura cross-coupling reaction (Bond and Sermon 1973; Sermon et al. 1979; Atnafu et al. 2016; Jie et al. 2009). Nanomedicine involves extensive use of gold NPs and nanorods for diagnosis and therapeutic purposes (Siddiqi and Husen 2017a; Llevot and Astruc 2012; Sánchez et al. 2012) as carriers for delivering drugs, antigens and genetic materials to targeting sites without any side effects (Madhusudhan et al. 2014; Dykman and Bogatyrev 2007; Pissuwan et al. 2011) and as drugs or diagnostic tools in the therapy of tumors and rheumatoid arthritis (Bhattacharya and Mukherjee 2008; Brown et al. 2008). They also find application in electronics, photonics, sensing and imaging (El-Sayed 2001; Husen and Siddiqi 2014b).

Among the various ways to synthesize AuNPs, the most common are the reduction of gold ions with reducing agents such as sodium borohydride, hydrazine, N,N-dimethylformamide, citrate, or other organic compounds (Zhang and Wu 2010; Rivas et al. 2001) followed by surface modification with a suitable capping agent to prevent aggregation of particles by electrostatic or physical repulsion (Erik et al. 2012). However, the use of such reducing agents may show environmental toxicity or pose biological risks. Therefore, utilization of nontoxic chemicals, environmentally benign solvent (water) and renewable materials (plant products), agriculture waste (banana peel) and/or living organisms (viruses, bacteria, fungi, algae), which would decrease the carcinogenic chemical waste and prevent pollution, are some of the key issues in the green chemistry research (Dahl et al. 2007; Siddiqi et al. 2016). The use of plant-based biomaterials or biomolecules to synthesize AuNPs is expected to cause a minimum quantity of hazardous waste and consume less energy, compared to the chemical synthesis methods.

Biosynthesis of AuNPs and gold nanorods (AuNRs) has several advantages such as simplicity and biocompatibility. Biomolecules act as the reducing and capping agents in the large-scale commercial production of AuNPs. Biosynthesis of AuNPs using naturally occurring gums has proved to be cost-effective, nontoxic and eco-friendly. Plant extracts, such as natural gums, may act as both the reducing and capping agents in AuNP synthesis.

Natural gums are considered to be the pathological products that ooze out following injury to the plant. Gums are hydrocolloids, which are hydrophilic in nature. These are effective water adsorbents and may be solubilized by water, producing viscous aqueous systems. On hydrolysis, gums yield a mixture of sugars and uronic acids (Choudhary and Pawar 2014). Most of them are heterogeneous polysaccharides

with complicated structures, which would vary depending on the source and their age and possess extremely high molecular masses. Owing to the presence of a large number of hydroxyl groups, water is bonded inside the molecular structure by hydrogen bonding and additionally within the voids created by the complex molecular configuration. Therefore, it is not possible to provide defined structural formulae of these biopolymers (Rana et al. 2011). Linear polysaccharides occupy extra space than the highly branched compounds of a similar mass.

Generally, gum exudates contain galacturonic acid, arabinose, uronic acids, galactose, rhamnose, protein, Mg and Ca as the major structural constituents and also mannose, glucose, protein, xylose and fat as the minor constituents. Natural gums are biodegradable, biocompatible, nontoxic, environment-friendly, having a low-cost and processing edible sources. Gums of different sources and their derivatives, represent a distinct group of polymers widely used in food industry, pharmacy and medicine and in the manufacture of cosmetics, textiles, adhesives, lithography, paints and paper (Bhardwaj et al. 2000; Rana et al. 2011; Mirhosseini and Amid 2012; Ibrahim et al. 2010; Prajapati et al. 2013a, b).

The plant-based naturally occurring gums, such as gum kondagogu, gum karaya, gum tragacanth, gum arabic, gum salmalia, guar gum, locust bean gum, gellan gum, xanthan gum, olibanum gum, gum katira, gum ghatti, bael gum and Prunus domestica gum, are used as the reducing and capping agents for fabrication of platinum, silver, gold and palladium NPs through green synthesis (Reddy et al. 2015a, b, c, 2017; Dhar et al. 2011; Atnafu et al. 2016; Saikat et al. 2012; Alam et al. 2017; Wu and Chen 2010; Pandey et al. 2013; Pooja et al. 2014; Rao et al. 2017; Huang et al. 2007a, b). Natural gums contain specific functional groups, such as -OH, -NH_2, -CHO, -$CONH_2$,-COOH, etc., which help in surface stabilization of NPs better than in other biological syntheses. Biosynthesis of AuNPs of various shapes and sizes by using various natural gums is shown in Table 4.1. The long polymer chain restricts the process of agglomeration of NPs. Therefore, NPs biosynthesized with natural gums were more stable through several months. The NPs stabilized with naturally occurring gums are harmless to cells and suitable for safe delivery of drugs, cancer detection and bio-imaging (Wu et al. 2006; Pooja et al. 2015). The attributes such as biocompatibility and antibacterial activity render the gold and silver NPs suitable as coating material in food packing and biomedical engineering. The present chapter is focused on green synthesis of AuNPs using natural gums and on their diverse applications.

4.2 Description of Various Gums

Gum kondagogu is a naturally available polysaccharide component extracted from the bark of *Cochlospermum gossypium* DC (family Bixaceae). It is made up of sugars such as galactose, arabinose, mannose, glucose, gluconic acid, rhamnose and galacturonic acid with sugar linkage of (1 → 6) β-D-Gal p, (1 → 2) β-D-Gal p, (1 → 2) α-L-Rha, 4-O-Me-α-D-Glc p A, (1 → 4) β-D-Glc p and (1 → 4) α-D-Gal p

Table 4.1 Gold nanoparticles of various size and shape synthesized by using the naturally occurring gums

Gum	Size	Shape	Reference
Bael gum	2 μm to 90 nm	Triangular	Subramanian et al. (2016)
Carboxymethyl Gum karaya	14 ± 2 nm	Spherical	Reddy et al. (2017)
Gellan gum	13 ± 1 nm	Spherical	Dhar et al. (2008)
Gellan gum	14 nm	Spherical	Dhar et al. (2011)
Gellan gum	47 ± 10 nm	Nanorods	Vieira et al. (2015)
Gum acacia	4–29 nm	Spherical	Reddy et al. (2015b)
Gum arabic	10 ± 2 nm	Spherical	Kattumuri et al. (2007)
Gum arabic	21.1 ± 4.6 nm	Spherical	Wu and Chen (2010)
Gum arabic	1.6 ± 0.7 nm	Spherical	Liu et al. (2013)
Gum arabic	4.045 ± 0.99 nm	Spherical	Joshita et al. (2014)
Gum arabic	Average size 5.5 nm	Spherical	Thanaa et al. (2015)
Gum ghatti	30 ± 1.2 nm	Spherical	Alam et al. (2017)
Guar gum	~6.5 nm	Spherical	Pandey et al. (2013)
Gum karaya	5.0 ± 1.2 nm	Spherical	Padil and Černík (2015)
Gum karaya	12 ± 2 nm	Spherical	Pooja et al. (2015)
Gum kondagogu	7.8 ± 2.3 nm	Spherical	Vinod et al. (2011)
Gum kondagogu	12 ± 2 nm	Spherical	Reddy et al. (2015a)
Gum kondagogu	4.08–12.73 ± 0.75 nm	Spherical	Selvi et al. (2017)
Katira gum	~6.9 nm	Spherical	Saikat et al. (2012)
Locust bean gum	16 ± 3 nm	Spherical	Tagad et al. (2014)
Olibanum gum	3 ± 2 nm	Spherical	Atnafu et al. (2016)
Prunus domestica gum	7–30 nm	Spherical	Islam et al. (2017)
Salmalia malabarica gum	12 ± 2 nm	Spherical	Reddy et al. (2015c)
Tamarind gum	50–150 nm	Spherical	Biswala et al. (2013)
Xanthan gum	15–20 nm	Spherical	Pooja et al. (2014)

A. It is an acidic gum and has carboxylic acid, acetyl, hydroxyl, and carbonyl groups as the major functional groups (Kumar and Ahuja 2012).

Gum karaya obtained from *Sterculia urens* Roxb. (family Sterculiaceae) is a highly branched acidic polysaccharide. The carbohydrate structure has the main chain of rhamnogalacturonan consisting of α-(1 → 4)-linked D-galacturonic acid and α-(1 → 2)-linked L-rhamnosyl residues. The side chain is composed of (1 → 3)-linked β-D-glucuronic acid, or (1 → 2)-linked β-D-galactose on the galacturonic acid unit, where one-half of the rhamnose is substituted by (1 → 4)-linked β-D-galactose (Galla and Dubasi 2010).

Gum tragacanth (GT) is a natural gum obtained from dried sap of several species of the genus *Astragalus* (e.g., *A. tragacantha*, *A. adscendens*, *A. gummifer* and *A. brachycalyx*). The gum contains pectinaceous arabinogalactans and fucose-substituted xylogalacturonans. It is a heterogeneous and acidic polysaccharide, which contains a mixture of two polysaccharides, of which the water-soluble component is called tragacanthin and the acidic water-swellable component is called

bassorin. The water-soluble tragacanthin is a neutral, highly branched arabinogalactan comprising (1 → 6)- and (1 → 3)-linked core chain with galactose and arabinose units and side groups of (1 → 2)-, (1 → 3)- and (1 → 5)-linked arabinose units occurring as monosaccharides or oligosaccharides. Bassorin, a pectic component, has a chain of (1 → 4)-linked α-D-galacturonic acid units, some of which are substituted at O-3 with β-D-xylopyranosyl units and some are terminated with D-Gal or L-Fuc (Kora and Arunachalam 2012).

Gum arabic, obtained from *Acacia nilotica* (L.) Willd. ex Delile (family Mimosaceae), is a slightly acidic or neutral polysaccharide complex obtained as a mixed magnesium, potassium and calcium salt. The backbone consists of 1 → 3-linked β-D-galactopyranosyl units, and the side chains contain units of β-D-glucuronopyranosyl, α-L-rhamnopyranosyl, α-L-arabinofuranosyl and 4-O-methyl-β-D-glucuronopyranosyl (Dror et al. 2006).

Gum salmalia extracted from the plant *Bombax ceiba* L. (former *Salmalia malabaricum*) (family Bombacaceae). On hydrolysis, it shows the presence of various sugars such as L-arabinose, D-galactose, D-galacturonic acid, rhamnose, thiamine, riboflavin, 2,3,5-tri- and 2,5-di-O-methyl-L-arabinose and 2,3,4,6-tetra-,2,6-di- and 2,4-di-O-methyl-D-galactose (Das et al. 1990).

Guar gum (GG) is a non-ionic edible polysaccharide derived from the seeds of *Cyamopsis tetragonolobus* (L.) Taub. (family Fabaceae). It consists of linear chains of (1, 4)-β-D-mannopyranosyl units with α-D-galactopyranosyl units attached via (1 → 6) linkages (Dodi et al. 2011).

Locust bean gum (LBG) is extracted from the endosperms of hard seeds of the locust bean tree, *Ceratonia siliqua* L. (family Fabaceae). It is a non-starch polysaccharide and polyhydroxylated biopolymer consisting of galactomannan units with mannose backbone and galactose units as single side chain (Dey et al. 2011).

Xanthan gum (XG) is a natural extracellular polysaccharide derived from a cabbage plant bacterium, known as *Xanthomonas campestris*, which is an anaerobic, gram-negative rod made up of penta saccharide repeat units, comprising glucose, mannose and glucuronic acid in the molar ratio 2.0:2.0:1.0 (Maity and Sa 2014).

Olibanum gum (OG) is obtained from *Boswellia serrata* Roxb. (family Burseraceae). Its chemical composition depends on its three principal areas of origin, Eritrea, Aden/Somalia, and India, which contains approximately 20–30% polysaccharides, 13–17% acid resin, 3–8% volatile oil and 40–60% boswellic acid (Kora et al. 2012).

Gellan gum (GG) is an anionic polysaccharide produced by a microorganism *Sphingomonas elodea*. It has a tetrasaccharide repeating unit composed of (1–4)-α-L-rhamnose, (1–4)-β-D-glucose and (1–3)-β-D-glucose and (1–4)-β-D-glucuronic acid as the backbone (Ahuja et al. 2013).

Katira gum (KG) is exuded from the *Cochlospermum religiosum* L. (Alston) (family Bixaceae) and consists of L-rhamnose, D-galactose and D-galacturonic acid in a molar ratio 3:2:1, together with traces of a ketohexose (Ojha et al. 2008).

Bael gum (BG) is obtained from fruits of *Aegle marmelos* L. Correa (family Rutaceae). Purified bael gum polysaccharides contain D-galacturonic acid (7%), L-arabinose (12.5%), D-galactose (71%) and L-rhamnose (6.5%) (Arati et al. 1976).

Prunus domestica gum (PDG) is isolated from the plum tree (*Prunus insititia* L. of the family Rosaceae) and contains L-arabinose, D-galactose and D-mannose, in a molar ratio of 3:2:1 and 3% of D-xylose (Islam et al. 2017).

4.3 Synthesis of AuNPs

In general, bioreduction of Au^{3+} with gum solution to form a ruby red color solution indicates the formation of AuNPs (Punuri et al. 2012). The size, shape, and morphology of AuNPs depend on the (i) concentration and volume of $HAuCl_4$ and gum, (ii) reaction time and (iii) pH medium of the solution. Brief procedure for fabrication of AuNPs involves mixing of various concentrations of gum solution with aliquot amount of precursor ($HAuCl_4$). The mixture is subjected to autoclaving or microwave irradiation or direct heating or ultra-sonication. The color of the resultant changes from yellow to ruby red indicating the formation of AuNPs, as depicted in Fig. 4.1. The major advantage of gum-capped AuNPs is that these NPs are more stable for several months without aggregation, owing to the presence of multifunctional groups and possess negative surface which acts as a stabilizing agent.

Dhar and his group demonstrated synthesis of AuNPs with gold ion solution heating with gellan gum; pH of the solution was adjusted to 11–12 with NaOH to

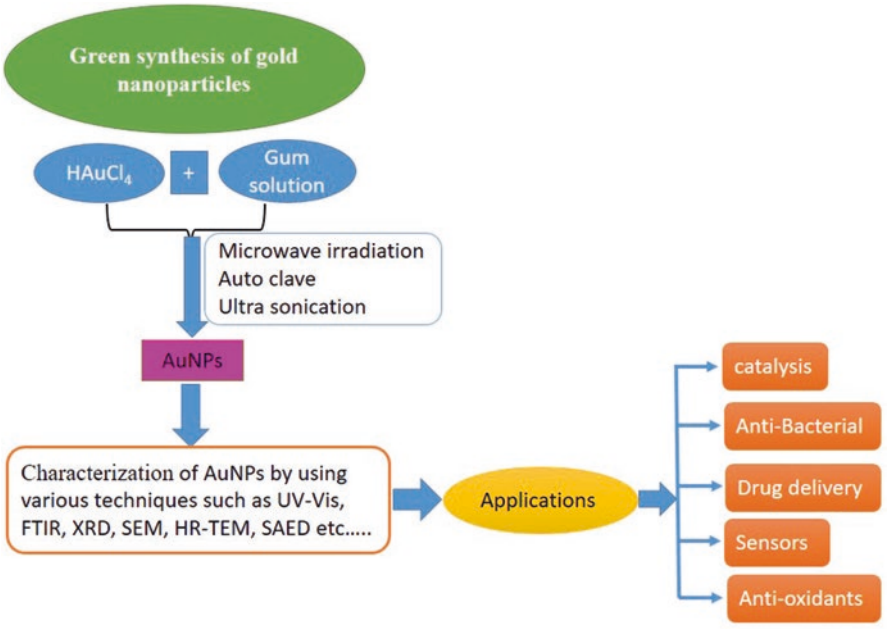

Fig. 4.1 Schematic representation of fabrication of AuNPs by using natural gums, their characterization and applications

yield ruby red AuNPs. Formation of AuNPs was confirmed by UV-Vis absorbance maximum at 520 nm. The TEM image reveals that NPs are well-dispersed with narrow size distribution and an average size of 13 ± 1 nm (Dhar et al. 2011). The SAED pattern of the AuNPs is indexed to the 111, 200, 220 and 311 Bragg reflections which represents a face-centered cubic (fcc) structure (Dhar et al. 2011). These gum-capped AuNPs have greater stability to pH and electrolyte changes relative to the citrate- and borohydride-reduced NPs (Dhar et al. 2011). Sílvia Vieira and coworkers developed layer-by-layer-coated gold nanorods (AuNRs) by using poly(acrylic acid), poly(allylamine hydrochloride), and gellan gum, which allowed formation of a GG hydrogel-like shell with 7 nm thickness around individual AuNPs. This method produces nanorods with an average length of 47 ± 10 nm (Vieira et al. 2015).

Gum kondagogu-stabilized AuNPs were prepared by mixing of gum solution with chloroauric acid in a boiling tube and kept in an autoclave at 120 °C and 15 psi pressure for 10 min (Reddy et al. 2015a), but the prepared NPs are larger in size (12 ± 2 nm) and of unequal shape. The surface plasma resonance (SPR) of prepared NPs exhibits at around 515–560 nm. The formation of NPs increases with increase in the concentration of gum, $HAuCl_4$ and autoclave time. FTIR spectra reveal that hydroxyl and carboxyl group peaks shifted from 3418 to 3445 cm^{-1} and 1606 to 1598 cm^{-1}, thus indicating the involvement of both the functional groups in the synthesis process. Vinod et al. (2011) showed that much smaller (7.8 ± 2.3 nm diameter) AuNPs could be produced from the reduction of $HAuCl_4$ with GK solution by using an orbital shaker at 75 °C, 250 rpm for 1 h. FTIR spectra indicate that hydroxyl functional group in the gum was responsible for the reduction of metal cation to NPs. UV-Vis analysis showed SPR at 525 nm due to the formation of AuNPs (Vinod et al. 2011).

Gold NPs of various sizes and shapes are fabricated by using heteropolysaccharide extracted from the gum of *Cochlospermum religiosum* (katira gum). In this method, small (6.9 nm) and mostly spherical, with a few having a rod-like or decahedral shape, NPs are produced from the aqueous polysaccharide solution mixed with $HAuCl_4$. This mixture was then heated at 70 °C with constant stirring with the help of a magnetic stirrer. A typical SPR band was obtained at 540 nm initiallyand after 6 h of the reaction time, SPR band shifted to 520 nm, beyond which no change in SPR band was observed. The fcc crystalline nature of these AuNPs was identified by XRD analysis and SAED pattern (Saikat et al. 2012).

GG-capped AuNPs are spherical in shape, 6.5 nm in size with d-spacing (HR-TEM) of 0.23, 0.20 and 0.14 nm, which reveals fcc crystal lattice with (111), (200) and (220) planes, and the same was further confirmed by SAED pattern in HR-TEM (Pandey et al. 2013). These NPs were prepared by mixing Au^{3+} ions with the guar gum solution of predefined concentration, added with few drops of NaOH solution. The resultant solution was then stirred gently at the desired temperature (80 °C) for 160 min to yield gold NPs. The formed AuNP SPR band at 539 nm and peak intensity of the resultant solution gradually increase with increase in time, indicating the formation of AuNPs.

LBG-stabilized AuNPs of various sizes and shapes are synthesized by employing the autoclave method, as described by Tagad et al. (2014). The AuNPs produced are spherical in shape and have the fcc crystal structure and SPR band at 537 nm. The authors of this procedure (Tagad et al. 2014) conclude that the hydroxyl groups and the hemiacetal reducing ends of LBG act as the active reaction centers to facilitate the reduction of Au^{3+} to Au^0 as shown in Fig. 4.2. This is further confirmed by FTIR spectra, which show a peak at 1728 cm^{-1} which arises from the carbonyl stretching vibrations at the reducing end of the gum after addition of Au^{3+} ions in the reaction mixture. The carbonyl functional groups at the ends of the gum chain get oxidized to the carboxyl group; increase in the peak intensity was observed at 1642 and 1554 cm^{-1} and the peak disappeared at 1728 cm^{-1}. It indicates that the reduction of Au^{3+} is coupled with the oxidation of hemiacetal/aldehyde groups in the formation of LBG-stabilized AuNPs.

Formation of the xanthan gum-capped AuNPs is monitored through various reaction parameters such as (i) reaction time, (ii) temperature, (iii) concentration and volume of gum solution and (iv) concentration and volume of gold solution. In this method, XG-capped NPs are prepared by heating the aqueous solution of $HAuCl_4$ at 80 °C in the presence of xanthan gum solution (1.5 mg mL^{-1}) with a reaction time of 3 h. The NPs produced show a mean particle size of 15–20 nm and a zeta potential of −47.2 ± 2.59 mV. These NPs are stable at a pH range of 5–9 and the NaCl concentration up to 0.5 M (Pooja et al. 2014). Muddineti et al. (2016) reported the synthesis of AuNPs by using ascorbic acid as the reducing agent and xanthan gum as the stabilizing agent. Synthesis of AuNPs was carried out by mixing xanthan gum with hydrogen tetrachloroaurate (III) hydrate, followed by addition of ascorbic acid to a mixture of xanthan gum Au^{3+} solution to form AuNPs. The effect of concentration of $HAuCl_4$, ascorbic acid and methoxy polyethylene glycol thiol (mPEG800-SH)

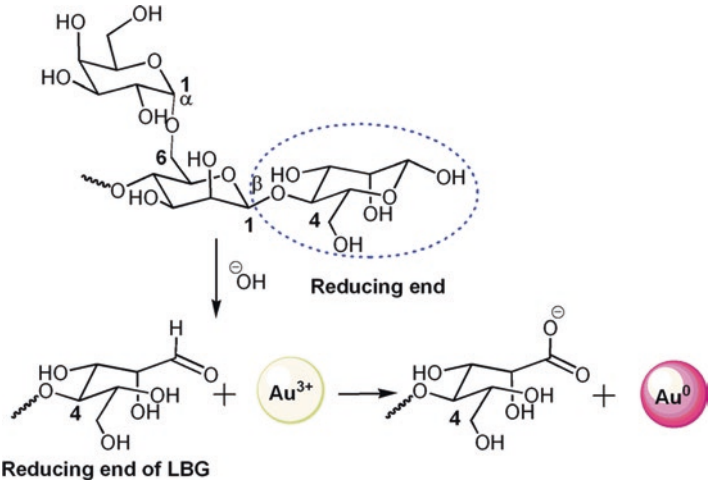

Fig. 4.2 LBG structure and reaction mechanism of AuNP synthesis at the reducing end of LBG biopolymer (Tagad et al. 2014)

was optimized. Stable AuNPs were formed at a concentration of 0.25 mM, 50 μM, and 1 mM for $HAuCl_4$, ascorbic acid and PEG-800SH, respectively. The so-produced AuNPs showed an absorption maximum at 540 nm and a hydrodynamic diameter of 80 ± 3 nm. During the reaction, the Au^{3+} ions were reduced to Au^0 (metallic gold) by using ascorbic acid. Au^0 atoms were further stabilized by the XG-coating and PEGylation, resulting in the formation of PX-AuNPs with improved stability. This is explained by the following chemical equation:

$$2HAuCl_4 + 3C_6H_8O_6 \rightarrow 2Au^O + 3C_6H_6O_6 + 8HCl$$

Gum acacia-stabilized AuNPs are prepared by mixing a homogeneous GA solution with chloroauric acid in a boiling tube and autoclaving at 121 °C and 15 psi pressure for 15 min. The NPs formed exhibit SPR within 520–550 nm. As the gum and chloroauric acid concentrations increase, formation of NPs also increases, as confirmed by the UV-Vis spectra. The NPs show fcc crystal structure and have the particle size around 4–29 nm. FTIR analysis reveals that –OH groups available in the gum matrix are responsible for reducing the $HAuCl_4$ to AuNPs (Reddy et al. 2015b). The authors also developed SMG-stabilized stable AuNPs with a particle size of 12 ± 2 nm, which is adjusted by varying the amounts of gum and chloroauric acid used in the NP synthesis. These NPs have SPR band around 520–530 nm and are highly crystalline in structure with fcc geometry. FTIR analysis indicates that –OH groups available in the gum matrix might be responsible for the reduction of Au^{3+}into AuNPs (Reddy et al. 2015c).

Likewise, one-step microwave-assisted green synthesis of well-stabilized AuNPs by reduction of $HAuCl_4$ with water-soluble olibanum gum was reported by Atnafu et al. (2016). Formation of AuNPs was confirmed with the help of UV-Vis, FTIR, XRD and TEM spectra. The fabricated NPs were well-dispersed and spherical in shape and their average diameter was around 3 ± 2 nm. The rate of NP formation increased and the NP size decreased when gum concentration and irradiation time were increased. The authors concluded that the –OH functional group of gum was responsible for the formation and stabilization of AuNPs.

Pooja et al. (2015) reported the synthesis and characterization of gum karaya (GK)-stabilized AuNPs. In this method GK solution is mixed with $HAuCl_4$ and stirred magnetically for 1 h at 90 °C. The solution color change from colorless to wine red at the absorbance of 536 nm indicates the formation of AuNPs. The observed particle size of optimized AuNPs is 91.7 nm with 0.389 PDI and −21.8 mV zeta potentialand particle size ranges between 20 and 25 nm, as determined by TEM. These authors also found that a 90 °C reaction temperature, 60 min reaction time, 2.5 mL of 15 mg mL^{-1} gum solution and 100μL of gold solution are the optimal conditions for the synthesis of NPs (Pooja et al. 2015). Carboxyl-methylated GK-capped AuNPs were prepared by Reddy et al. (2017). Carboxymethyl gum-capped AuNPs are smaller in size (14 ± 2 nm), compared to normal gum-capped AuNPs because carboxymethyl gum is a more effective capping agent than the normal gum. As the gum is converted to carboxymethyl gum, its solubility increases and NP formation accelerates (Reddy et al. 2017).

A facile and complete green synthesis of AuNPs by gum arabic was reported by Wu and Chen (2010). Various concentrations of hydrogen tetrachloroaurate (0.1, 0.3, 0.5, 0.7, and 0.9 mM) were mixed with concentrations (1, 5, 10, 15, and 20 mg mL^{-1}) of arabic gum solution and stirred gently at the desired temperatures (25, 40, 55, and 70 °C) to yield AuNPs. The synthesis reaction was finished in 2–4 h. Increase in the reaction temperature increased the NP formation rate but had no significant effect on the optical property and the size of AuNPs. The particle size distribution was broader at a higher Au^{3+} ion concentration or a lower gum arabic concentration due to insufficient protection. A too high gum arabic concentration was not suitable for stabilization of AuNPs because the increased intermolecular force of the gum arabic might hinder the dispersion of AuNPs.

The use of gum ghatti for reduction, stabilization and surface functionalization during the synthesis of stable AuNPs was reported by Alam et al. (2017). In this method, preheated gum solution was added dropwise to a required volume of $HAuCl_4$ (0.1 M) under constant stirring until the color changed from yellow to ruby red color, which indicated the formation of AuNPs. The synthesized and optimized AuNPs were spherical, having SPR band at 530 nm, DLS for its hydrodynamic size (112.5 nm), PDI (0.222), and zeta potential (−21.3 mV). The authors explained that a 4% of gum solution was just sufficient for nucleation, moderate size and growth; temperature above 60 °C ensured the best performance.

Gum tragacanth-stabilized AuNPs were prepared by mixing gum solution with gold solution and magnetically stirred (150 rpm) for 4 h at 65 °C. The resultant solution had SPR at 548 nmand synthesis of GT-AuNPs was optimized by changing various parameters like concentration and volume of GT and gold solutions. The maximum absorbance of SPR was observed for 5 mg mL^{-1} GT and 5 mM gold solution concentrations. GT-capped AuNPs were stable against salt concentration, pH and plasma contact time (Rao et al. 2017).

An interesting study by Subramanian et al. (2016) illustrated an eco-friendly and selective synthesis of triangular AuNPs by the reduction of $HAuCl_4$ with bael gum (*Aegle marmelos* gum); the NPs were in the range of 92 ± 20 nm. The size and shape (such as triangular with a tail, triangular, triangular truncated at the apex, and hexagonal) depend on the concentration of bael gum and reaction temperature. The concentration ratio of bael gum and $HAuCl_4$ for the reduction of $HAuCl_4$ 1:1 at 30 °C was very slow and resulted in the formation of plates largely triangular, but the ratio increment 1:2.5 at 30 °C formed the polydispersed AuNPs with tail. Further increment in ratio (1:4) at room temperature gave perfect nanoplates (triangular as well as hexagonal) of ≈ 2 μm. The increase in weight percentage of bael gum from 1:7 to 1:12.5 led to a reduction in size from ≈ 1 μm to ≈ 500 nm. In this stage, predominantly 67% of NPs were hexagonal in shape, the rest being triangular and truncated triangular. Further increase in the concentration of bael gum gave rise to spherical AuNPs with average size 20 nm. At fixed bael gum and $HAuCl_4$ concentrations, the NP size was 260 ± 66 nm at 50 °C and 92 ± 20 nm at 70 °C. This suggests that 1:10 ratio of $HAuCl_4$ and bael gum forms pure triangular NPs at 70 °C and spherical AuNPs at more than 90 °C.

4.3.1 Reaction Mechanism

The naturally occurring gums act as a reducing agent for gold ions and a capping agent after the formation of AuNPs. The generally accepted mechanism for fabrication of AuNPs involves a two-step process, i.e., atom formation and then polymerization of the atom. In the first step, gum solution is heated by various means such as autoclaving, microwave irradiation, normal heating, or sonochemical treatment. The biopolymer obtained may expand and become more accessible for gold ions to interact with the available functional groups of gums. Gums contain carbohydrate polymers such as rhamnose, galactose and uranic acid and the functional groups such as hydroxyl, carbonyl and carboxyl groups. Compared to other biopolymers, a gum is an anionic functional group with a greater charge density. The presence of negatively charged groups is also confirmed from the negative zeta potential value for the gum. This negative charge facilitates the attraction of positively charged gold ion to the polymeric chain. Subsequently, these gold ions oxidize the hydroxyl and carbonyl groups to carboxyl group and conversely get themselves reduced to gold atoms. In addition to this inherent oxidation, the dissolved air also causes oxidation of the existing hydroxyl groups to carbonyl (-CHO and -COOH) groups. In turn, these powerful reducing aldehyde groups, along with the other abundantly present carbonyl groups, reduce more and more of the gold ions to gold atoms. In the second step, these NPs are capped and stabilized by the polysaccharides present in the gum. The stabilization of AuNPs occurs through a strong association between AuNP surface and "O" atoms of the hydroxyl and carbonyl functional groups of the natural gums. The resulting stabilized AuNPs avoid coalescing with the neighboring one due to the electrostatic repulsion and steric effect (Tagad et al. 2014; Vinod et al. 2011; Subramanian et al. 2016; Pandey et al. 2013; Selvi et al. 2017).

4.4 Characterization of AuNPs

Synthesized NPs are characterized by using various techniques such as UV-Vis spectroscopy, FTIR spectroscopy, X-ray diffraction (XRD), scanning electron microscopy (SEM), TEM, selected area electron diffraction (SAED) and dynamic light scattering (DLS) zeta potential. These techniques are useful to determine the crystal structure, size, shape, charge, disparity, surface area and surface modification of NPs.

UV-Vis spectroscopy is a simple and sensitive technique for the characterization of AuNPs due to its extension to SPR. In general trend, SPR band shows a red shift with increasing particle size, while aggregation of colloidal gold causes a decrease in the intensity of the main peak and also results in a long tail on the long-wavelength side of the peak. The shape-dependent radioactive properties of metallic particles can be treated by the Gans modification of Mie theory, which predicts that a shift in the SPR occurs when particles deviate from spherical geometry. In this condition,

the longitudinal and transverse dipole polarizability no longer produces equivalent resonances. Therefore, there appear two plasma resonances: a broadened and red-shifted longitudinal plasmon resonance and a transverse plasmon resonance. For example, gold nanorods (AuNRs) exhibit two plasmon bands: strong longitudinal band in the near-IR region and a weak transverse band, similar to that of spherical AuNPs (520 nm), in the visible region. The resonance of the longitudinal mode, a red shift and strong, depends on the aspect ratio (defined as the ratio of the length to width of the rod) of the nanorods. An absorption spectrum of colloidal AuNRs (with accepted ratio 4:1), showing the presence of two absorption maxima, is presented in Fig. 4.3a. The spherical AuNPs show only one SPR around 500–600 nm (Fig. 4.3b), and this is attributed to the oscillation of the conduction band electrons induced by the interacting electromagnetic field with the concerned metallic NPs (Saha et al. 2012; Huang and El-sayed 2010; Daniel and Astruc 2004; Mayer and Hafner 2011).

In order to monitor the effect of different parameters to the formation of AuNPs, the UV-Vis absorption spectra of synthesized AuNPs were recorded against various parameters such as gum concentration, $HAuCl_4$ and reaction time. The SPR absorption band appears approximately at 500–600 nm, which is associated with the formation of AuNPs. The efficacy of the formation of AuNPs increases with increase in the concentration of gum at fixed concentration of $HAuCl_4$. Further increase in the concentration of gum results in a decrease in the peak intensity and the peaks shifted toward longer wavelength are shown in Fig. 4.4a. The production of AuNPs with different concentrations of $HAuCl_4$ and reaction times with fixed concentration of gum is shown in Fig. 4.4b. It can be observed that the strong absorption band increases with increase in concentration and reaction time. The stability of synthesized NPs was monitored at different pH values, electrolytes, and reaction times. The red shift, normally observed in UV-Vis spectra, is an indication of agglomeration of NPs or increase in the size of the particle or both. The synthesized NPs did not show any shift in the peak, which indicates that NPs are stable and aggregation of gold NPs is protected by the gum.

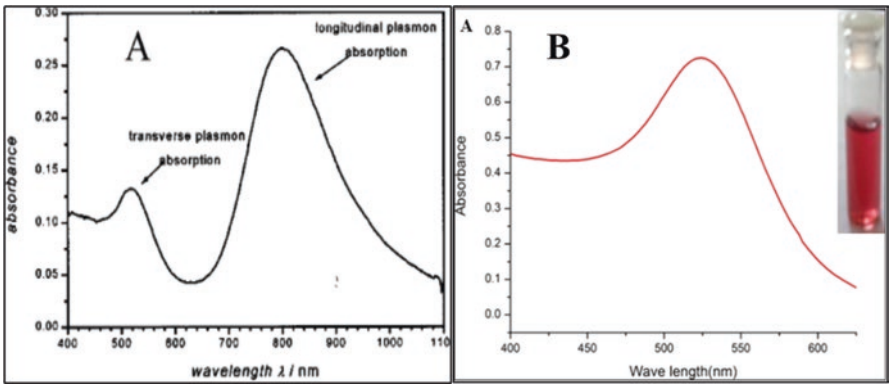

Fig. 4.3 UV-Vis absorption spectra of (**a**) gold nanorods (Ghosh and Pal 2007), (**b**) gold nanoparticles (Madhusudhan et al. 2014)

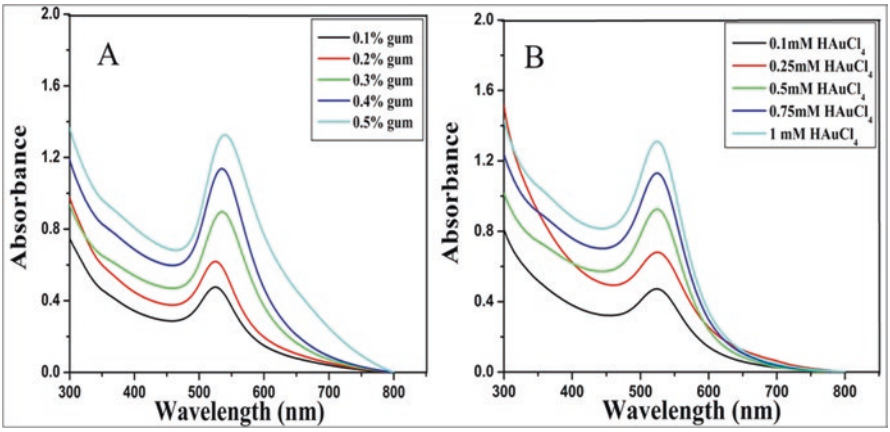

Fig. 4.4 UV-Vis absorption spectra of the AuNPs synthesized: (**a**) different concentrations of olibanum gum solution containing 1 mM $HAuCl_4$ by MWI 9 min and (**b**) different concentrations of $HAuCl_4$ solution containing 0.5% olibanum gum by MWI 9 min (Atnafu et al. 2016)

The active sites on natural gums involved in the reduction of gold ions and AuNP formation were investigated by using the Fourier-transform infrared (FTIR) spectroscopy. The obtained aqueous AuNP dispersion was first centrifuged or lyophilized, and then the sample was used for FTIR analysis, prepared in the form of a thin transparent pellet with potassium bromide (KBr). A pure KBr was used as a background and the same was subtracted from the FTIR spectra of the gum-capped AuNPs. The FTIR spectra were recorded with a scanning range from 400 to 4000 cm^{-1}. The interaction between gum and AuNPs through hydroxyl and carbonyl groups showed the stretching vibration of hydroxyl group at 3445 cm^{-1}, carbonyl stretching vibration at 1722 cm^{-1}, and asymmetric stretch of carboxylate group at 1606 cm^{-1} (Reddy et al. 2015a). After the formation of AuNPs, the peaks for hydroxyl group and asymmetric stretch of carboxyl group were shifted from 3418 to 3445 cm^{-1} and from 1606 to 1598 cm^{-1}, respectively, in comparison with those in the native gum kondagogu, suggesting that both hydroxyl and carbonyl functional groups were involved in the synthesis and stabilization of AuNPs (Fig. 4.5). In another study, Atnafu et al. (2016) demonstrated that the FTIR spectra of olibanum gum show major peaks located at 3421, 2932, 1726, 1427, 1244 and 1033 cm^{-1}. The peaks 3421 and 2932 cm^{-1} can be assigned to the stretching vibration of the hydroxyl and methylene group. The bands observed at 1726, 1617 and 1427 cm^{-1} could be attributed to the characteristic asymmetrical and symmetrical stretches of the CO_2^- (carboxylate ion) group connected to the olibanum gum. The absorption bands of the olibanum gum-capped AuNPs were detected at 3356, 2932, 1719, 1595, 1448, 1259 and 1065 cm^{-1}. These peaks were shifted from 3421 to 3356, 1726 to 1719, 1617 to 1595, and 1427 to 1438 cm^{-1} when compared to those in the native olibanum gum, and other peaks were found to remain unchanged. Rao et al. (2017) reported that –OH, –C=O and –C–O functional groups of gum tragacanth are actively involved in the reduction and stabilization of AuNPs. These

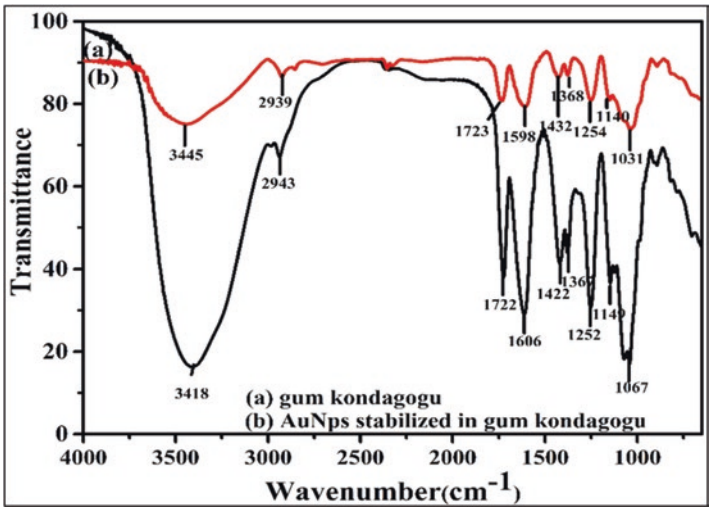

Fig. 4.5 FTIR spectra of (a) gum kondagogu and (b) AuNPs stabilized in gum kondagogu (Reddy et al. 2015a)

results indicated that hydroxyl groups and the carboxyl groups were involved in the synthesis and stabilization of AuNPs. In general, formation of AuNPs is a two-step process. In the first step, gum containing hydroxyl functional group is oxidized to form carbonyl functional group, and gold ion is reduced to gold atom. In the second step, the oxygen atom which is present in the functional carbonyl and hydroxyl groups helps in forming the lid to protect aggregation of NPs as it has a strong association with the AuNPs.

The shape, size and surface morphology of NPs are studied microscopically using the SEM, FE-SEM, TEM and AFM techniques. Among all these, TEM has the maximum magnification and resolution. To understand better the effects of synthesis conditions on the size and shape of AuNPs, TEM was used to evaluate the morphology and size of some representative AuNPs obtained. In order to estimate the effect of capping nature of gum extract over the growth and formation of AuNPs, experiments were conducted with different concentrations (0.1 and 0.5%) of olibanum gum with fixed concentration of precursor (1 mM $HAuCl_4$) and 9 min microwave irradiation (MWI) time (Atnafu et al. 2016), as shown in Fig. 4.6a, c. The prepared NPs were found to be spherical in shape and well-dispersed in the gum matrix. The average particle diameter obtained from these micrographs was about 8 ± 2 (0.1% olibanum gum) to 3 ± 4 nm (0.5% olibanum gum) as shown in Fig. 4.6b, d. These findings clearly indicate that as the concentration of gum increases from 0.1% to 0.5%, the average size of the AuNPs formed decreases.

The selected area electron diffraction (SAED) pattern, which exhibited diffused ring pattern, indicates that these AuNPs are highly polycrystalline in nature. The four rings associated with the pattern can be ascribed to the diffraction from (111), (200), (220) and (311) lattice planes of the face-centered cubic (fcc) gold (Fig. 4.7a).

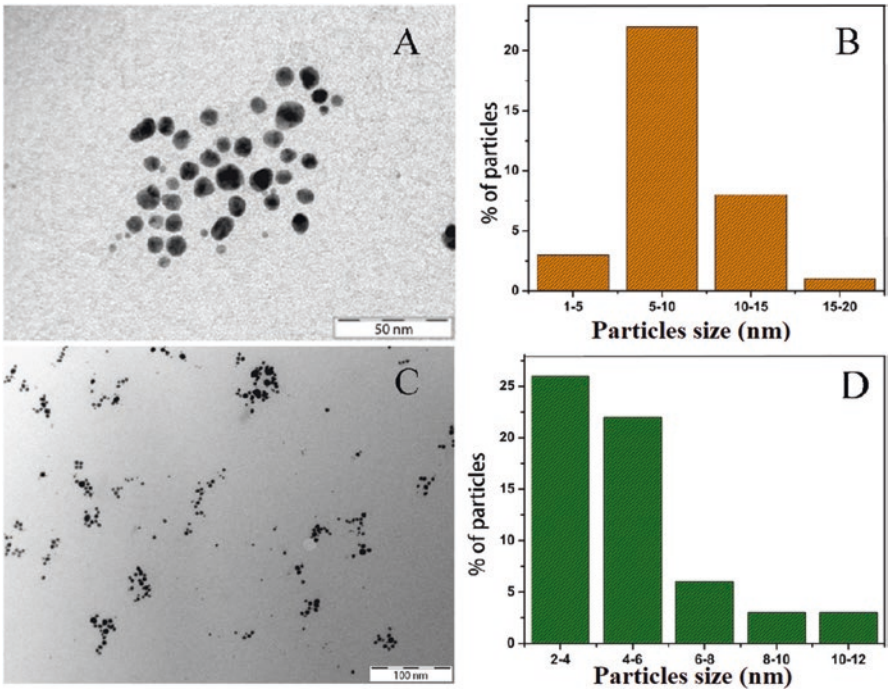

Fig. 4.6 TEM photomicrographs showing (**a**) 0.1% olibanum gum, 1 mM $HAuCl_4$, and 9 min MWI time and (**c**) 0.5% olibanum gum, 1 mM of $HAuCl_4$, and 9 min MWI time. The (**b**) and (**d**) are histograms of the particle size distribution of 0.1% and 0.5% of gum (Atnafu et al. 2016)

Subramanian et al. (2016) demonstrated that the size and shape of NPs depend critically on the concentration of the bael gum. The bael gum-capped NPs with triangular, triangular with truncation at the apex, and hexagonal plates are the predominant shapes over a wide concentration range, at room temperature. At higher concentration of bael gum and at room temperature, the NPs are spherical. However, fine-tuning of temperature, at a particular concentration of bael gum, leads to the formation of perfect triangular NPs, as shown in Fig. 4.7b. Rao et al. (2017) determined the shape and morphology of NPs through AFM microscopy and established that the prepared NPs were spherical in shape with nano-range size and stabilized by the multifunctional groups of gum tragacanth.

4.4.1 EDX Analysis

The presence of Au atoms in the gum-capped AuNPs was confirmed by Reddy et al. (2015c) and Atnafu et al. (2016), using the energy-dispersive X-ray analysis (EDXA), which gives additional evidence for the reduction of $HAuCl_4$ into

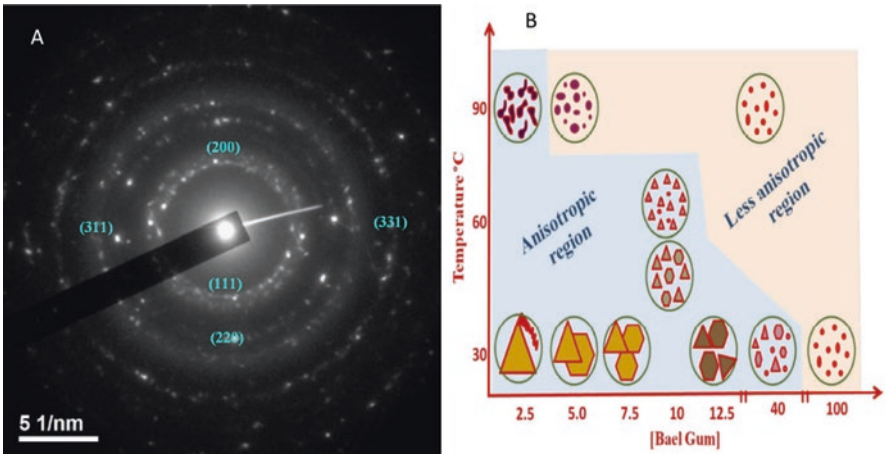

Fig. 4.7 (**a**) SAED patterns of AuNPs prepared by using katira gum (Saikat et al. 2012). (**b**) Representation of the shape of nanoparticles as a function of temperature and weight formation of AuNPs by using bael gum (Subramanian et al. 2016)

elemental gold. Of late, Islam and associates explained EDX analysis of the *Prunus domestica* gum-loaded AuNPs. These NPs showed strong peaks at 0.6 and 2.6 keV, while a weak signal was observed at 9.7 keV (Islam et al. 2017). The other strong signals for C and O were also there due to the presence of bioorganic molecules capping the gold NPs.

4.4.2 Dynamic Light Scattering (DLS)

Dynamic light scattering (DLS) is the most versatile and useful set of techniques for measuring the average particle size and zeta potential. It was observed that the obtained DLS and TEM differ considerably for small AuNPs. While TEM gives the diameter of the individual NPs, DLS also takes the capping shell into account, thus providing information on the size of the whole conjugate. In suspensions of small AuNPs, the number of saccharide molecules per particle is high, and hence the hydrodynamic size obtained from DLS is greater than that obtained by TEM. The stability and surface charge of synthesized AuNPs were also studied by zeta potential. Particles with highly negative or positive surface charge are considered to be stable. An absolute zeta potential value of ±30 mV is a general indication that the colloidal solution is highly stable (Venkatpurwar et al. 2011; Sankar et al. 2017). Reddy et al. (2015b) reported that the gum acacia-stabilized AuNPs have an average particle size of about 24.29 nm and zeta potential value of −29.3 mV, as shown in Fig. 4.8. These results indicate that AuNPs capped with gum acacia carried negatively charged groups and were dispersed in the medium, proving that they were stable. Pooja et al. (2014) demonstrated that the xanthan gum-stabilized AuNPs had

a mean hydrodynamic diameter of 41 ± 3.78 nm. The NPs showed a high poly-dispersity (0.35–0.6), which can be attributed to the presence of a wide range of particles. The high negative surface potential (−47.2 ± 2.59) indicated a high stability of NPs in the presence of gum molecules.

4.4.3 XRD Analysis

The XRD technique is used to determine and confirm the crystalline structure of fabricated AuNPs. XRD pattern of the gum-capped AuNPs is shown in Fig. 4.9. In a study of Reddy et al. (2015a), AuNPs exhibited four well-defined peaks at 2θ = 38.1, 44.3, 64.5 and 77.7. All the four peaks correspond to standard Bragg reflections for (111), (200), (220) and (311) planes of the face center cubic (fcc) crystal structure of metallic gold. The existence of diffraction peaks was matched with the standard data files (the JCPDS card No. 04–0784) for all reflections. Furthermore, no extra peaks were found in XRD spectrum, indicating the high purity of the resultant AuNPs. The diffraction peak at 38.1 was a highly intense peak among the peaks observed. Saikat et al. (2012) (katira gum-capped AuNPs), Tagad et al. (2014) (locust bean gum-capped AuNPs), Islam et al. (2017) (*Prunus domestica* gum-stabilized AuNPs) and Reddy et al. (2015c) (*Salmalia malabarica* gum-capped AuNPs) reported similar findings on the formation of AuNPs. The mean particle diameter of AuNPs was calculated by using XRD data. AuNP diameter was derived by using Debye Scherer's formula ($D = k\,\lambda / \beta½ \cos\theta$), which exploits the reference peak width at an angle θ, where λ is the X-ray wavelength (1.5418), $\beta½$ is

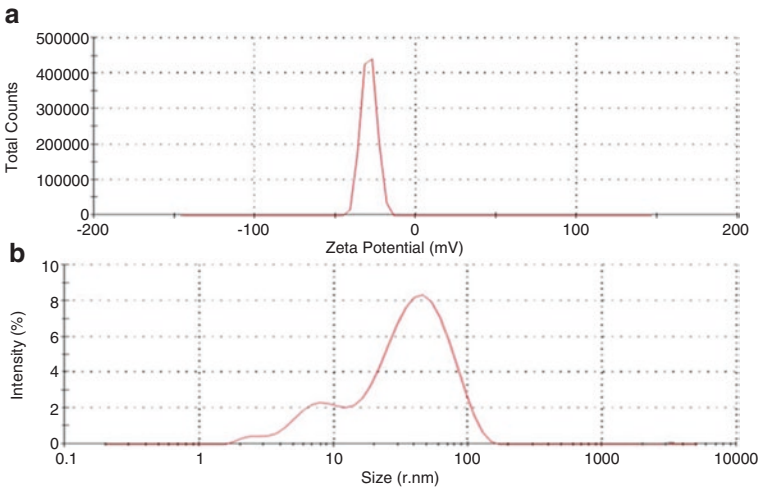

Fig. 4.8 (**a**) Zeta potential and (**b**) Zeta sizer distribution of the AuNPs with gum acacia (Reddy 2015b)

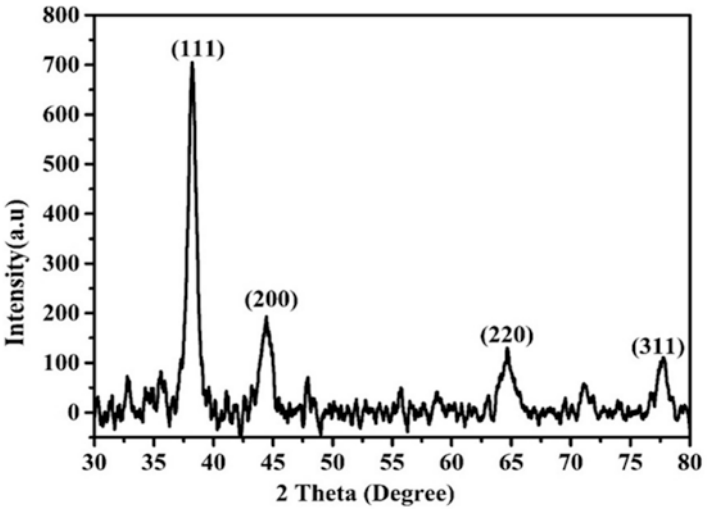

Fig. 4.9 XRD pattern of AuNPs stabilized by gum kondagogu (Reddy et al. 2015a)

the width of the XRD peak at half height and k is the shape factor. Average diameter of particle was 20 nm for the *Prunus domestica* gum-stabilized AuNPs, 13.2 nm for the *Salmalia malabarica* gum-capped AuNPs, and 13.1 nm for the gum kondagogu-capped AuNPs.

4.5 Applications

AuNPs have attracted a widespread interest due to their distinctive electrical and optical properties, such as unique and tunable SPR, surface-enhanced emission and surface-enhanced Raman scattering. Convenient and easy approach for particle size modification throughout the synthesis process and surface functionalization with different kinds of materials adds to the researcher's interest. The AuNPs remained largely overlooked till the 1850's, as they were used merely to decorate ceramics and glass. Until the Middle Ages, the soluble gold was used to disclose fabulous curative powers for various diseases, such as venereal problems, dysentery and tumors, and for diagnosis of syphilis (Dykman and Khlebtsov 2011, 2012). Thus, the remarkable features exhibited by colloidal gold have been utilized for centuries. Now, the advancement in synthesis and surface functionalization of AuNPs has led to various promising applications. Recent reports suggest that AuNPs capped with natural gums are being used in the fields of drug delivery, catalysis, antimicrobial activity, colorimetric metal ion detection and antiproliferative and vapor sensing.

Gold NPs are one of the most commonly explored and used carriers for the delivery of anticancer drug, such as doxorubicin hydrochloride (DOX), due to their controlled size, shape, surface functionality, improved efficacy and target specificity.

Dhar et al. (2008) demonstrated that gellan gum (GG)-capped most stable AuNPs have been used as carriers for the delivery of the cationic anthracycline drug, DOX, with a loading efficiency of about 75%. The reduction in zeta potential value from −38.25 to −30.00 mV indicates the electrostatic stability due to interaction between cationic DOX and anionic GG components in the DOX-loaded GG-AuNPs. DOX-loaded AuNPs are stable at different pH levels ranging from 4.0 to 8.0. Pooja et al. (2014) reported that the DOX-loaded AuNPs capped with xanthan gum were stable under different pH, electrolyte and serum conditions. Drug loading takes place on the surface of NPs due to interaction between the positive-charged amine group of DOX and the negative acidic group of gum, which was confirmed by the decrease in the surface charge to −29.1 ± 2.78 mV.

The study by Rao et al. (2017) suggests that gum tragacanth-capped AuNPs cargos increase the therapeutic efficiency of naringin by enhancing its bactericidal activity through their destabilizing effect on the bacterial surface morphology. Gum arabic-capped small-sized AuNPs can be used as a photothermal agent, which exhibits a strong photothermal effect for killing cancer cells, as reported by Liu et al. (2013).

The distinctive properties of AuNPs allow their use in the detection of copper metal, which was an identified potable and surface water contaminant. Carboxymethyl gum karaya (CMGK)-functionalized AuNPs were reported for the sensitive and selective detection of Cu^{2+} in aqueous solution, in the presence of 13 other metal ions. The Cu^{2+} sensing relies on the aggregation of CMGK-capped AuNPs owing to the addition of Cu^{2+} resulting in an increase in absorbance of NPs at 647 nm and a change in their color from red to blue (Reddy et al. 2017).

The guar gum-capped AuNPs were exploited for optical sensor applications for detecting the aqueous ammonia based on SPR. The developed method is found to be simple, with low cost, low detection limit of 1 ppb, high sensitivity and great reproducibility (Pandey et al. 2013). Locust bean gum (LBG)-stabilized AuNPs were doped in SnO_2 matrix and their utilization for ethanol vapor sensing was investigated. LBG-capped AuNPs doped in SnO_2 showed a fast response (~5 s) and good ethanol sensing behavior in the range of 10–120 ppm at room temperature (Tagad et al. 2014).

Gold NPs exhibit antibacterial activity by directly interacting with the bacteria cell walls and cause lysis. The antibacterial effect of AuNPs mostly depends on the size of particles; NPs smaller than 10 nm have a direct interaction with the bacteria and produce electronic effects, which enhance the reactivity of NPs. Reddy et al. (2015a) suggested that gram-negative strains of bacteria (*E. coli*) with thin cell walls are more susceptible to cell wall damage, compared to gram-positive strain bacteria (*B. subtilis*) with a thick cell wall. Islam et al. (2017) demonstrated that *Prunus domestica* gum-stabilized gold and silver NPs show antibacterial activity against gram-positive strains of *S. aureus* and gram-negative strains of *E. coli* and *P. aeruginosa*, but AuNPs are less effective compared to AgNPs.

Gold NPs possess a large surface area and high surface energy, making them the best catalysts in many reactions such as reduction of methylene blue (MB), Congo red (CR) and reduction of p-nitrophenol (4-NP) to p-aminophenol (4-AP). The cata-

lytic activity of synthesized AuNPs using gum kondagogu, gum acacia, katira gum locust bean gum, and olibanum gum was established in the reduction of 4-NP to 4-AP in the presence of $NaBH_4$. The rate of reduction was influenced by parameters such as concentration of AuNPs and reaction temperature (Reddy et al. 2015a, b; Saikat et al. 2012; Tagad et al. 2014; Atnafu et al. 2016).

The SMG-capped AuNPs operate through the mechanism of electron relay effect and accomplish the reduction of MB dye in 9 min and CR dye in 10 min in the presence of $NaBH_4$ (Reddy et al. 2015c). The catalytic electron transfer reaction between $K_3[Fe(CN)_6]$ and $NaBH_4$, resulting in the formation of $K_4[Fe(CN)_6]$ and dihydrogen borate ion, is effectively carried out in the presence of acacia gum-capped AuNPs and this reaction depends upon the concentration of AuNPs and temperature. Similar results were obtained for the olibanum gum-capped AuNPs (Reddy et al. 2015b; Atnafu et al. 2016).

4.6 Conclusion

Fabrication of AuNPs accomplished by using natural gums is nonhazardous, cost-effective, renewableand eco-friendly, compared to conventional methods. These gums serve the role of self-reducing and capping agents and thus the hazards associated with the use of additional capping agents are avoided. Gold NPs with controlled size and shape were obtained simply by varying the ratio of $HAuCl_4$ to gum concentrations. Gum-capped AuNPs are relatively more stable and do not show any sign of agglomeration even after storage for several months at room temperature, compared to those prepared through other bioreduction methods. Gums are capable to reduce metal ions faster than other bioreduction materials. Furthermore, in the scale-up industrial production of well-dispersed AuNPs, naturally occurring gums are certainly better than other bioreduction materials. Gum-capped gold NPs are more effective in a range of applications including catalysis, diagnosis, photonics and therapeutics due to their novel properties, biocompatibility and low toxicity.

References

Ahuja M, Singh S, Kumar A (2013) Evaluation of carboxymethyl gellan gum as a mucoadhesive polymer. Int J Biol Macromol 53:114–121

Alam MS, Garg A, Pottoo FH, Saifullah MK, Tareq AI, Manzoor O, Mohsin M, Javed MN (2017) Gum ghatti mediated, one pot green synthesis of optimized gold nanoparticles: investigation of process-variables impact using *Box-Behnken* based statistical design. Int J Biol Macromol 104:758–767

Arati R, Bhattacharya SB, Mukherjee AK, Rao CVN (1976) The structure of degraded bael (*Aegle marmelos*) gum. Carbohydr Res 50:87–96

Atnafu GA, Ayal AM, Akele ML, Addis KA, Reddy GB, Veerabhadram G, Madhusudhan A (2016) Microwave-assisted green synthesis of gold nanoparticles using olibanum gum (*Boswellia ser-*

rata) and its catalytic reduction of 4-Nitrophenol and Hexacyanoferrate (III) by sodium borohydride. J Clust Sci 28:917–935
Reddy GB, Madhusudhan A, Ramakrishna D, Ayodhya D, Veerabhadram G (2015a) Green chemistry approach for the synthesis of gold nanoparticles with gum kondagogu: characterization, catalytic and antibacterial activity. J Nanostruct Chem 5:185–193
Reddy GB, Madhusudhan A, Ramakrishna D, Ayodhya D, Veerabhadram G (2015b) Catalytic reduction of p-Nitrophenol and Hexacyanoferrate (III) by borohydride using green synthesized gold nanoparticles. J Chin Chem Soc 62:420–428
Reddy GB, Madhusudhan A, Ramakrishna D, Ayodhya D, Veerabhadram G (2015c) Catalytic reduction of methylene blue and Congo red dyes using green synthesized gold nanoparticles capped by salmalia malabarica gum. Int Nano Lett 5:215–222
Reddy GB, Rajkumar B, Ramakrishna D, Girija MK, Veerabhadram G (2017) Facile green synthesis of gold nanoparticles with carboxymethyl gum karaya, selective and sensitive colorimetric detection of copper (II) ions. J Clust Sci 28:2873–2890
Bhardwaj TR, Kanwar M, Lal R, Gupta A (2000) Natural gums and modified natural gums as sustained-release carriers. Drug Dev Ind Pharm 26:1025–1038
Bhattacharya R, Mukherjee P (2008) Biological properties of "naked" metal nanoparticles. Adv Drug Deliv Rev 60:1289–1306
Biswala SK, Parida UK, Bindhani BK (2013) Gold nanoparticles capped with tamarind seed polysaccharide blended with chitosan composite for the growth of phosphate mineral. Int J Cur Eng Tech 3:1104–1108
Bogunia-Kubik K, Sugisaka M (2002) From molecular biology to nanotechnology and nanomedicine. Biosystems 65:123–138
Bond GC, Sermon PA (1973) Gold catalysts for olefin hydrogenation. Gold Bull 6:102–105
Brown CL, Whitehouse MW, Tiekink ERT, Bushell GR (2008) Colloidal metallic gold is not bioinert. Inflammopharmacology 16:133–137
Choudhary PD, Pawar HA (2014) Recently investigated natural gums and mucilages as pharmaceutical excipients: an overview. J Pharm 2014:204849
Corma A, Serna P (2006) Chemo selective hydrogenation of nitro compounds with supported gold catalysts. Science 313:332–334
Dahl JA, Maddux BLS, Hutchison JE (2007) Toward greener nano synthesis. Chem Rev 107:2228–2269
Daniel MC, Astruc D (2004) Gold nanoparticles: assembly, supramolecular chemistry, quantum-size-related properties, and applications toward biology, catalysis, and nanotechnology. Chem Rev 104:293–346
Das S, Ghosal PK, Ray B (1990) Structural studies of a polysaccharide from the seeds of *salmalia malabarica*. Carbohydr Res 207:336–339
Dey P, Sa B, Maiti S (2011) Carboxymethyl ethers of locust bean gum a review. Int J Pharm Pharm Sci 2:4–7
Dhar S, Maheswara Reddy E, Shiras A, Pokharkar V, Prasad BLV (2008) Natural gum reduced/stabilized gold nanoparticles for drug delivery formulations. Chem Eur J 14:10244–10250
Dhar S, Mali V, Bodhankar S, Shiras A, Prasad BL, Pokharkar V (2011) Biocompatible gellan gum-reduced gold nanoparticles: cellular uptake and subacute oral toxicity studies. J Appl Toxicol 31(5):411–420
Dimitratos N, Lopez-Sanchez JA, Hutchings JG (2012) Selective liquid phase oxidation with supported metal nanoparticles. Chem Sci 3:20–44
Dodi G, Hritcu D, Popa MI (2011) Carboxyl methylation of guar gum: synthesis and characterization. Cellulose Chem Technol 45:171–176
Dror Y, Cohen Y, Yerushalmi-rozen R (2006) Structure of gum arabic in aqueous solution. J Polym Sci Part B Polym Phys 44:3265–3271
Dykman LA, Bogatyrev VA (2007) Gold nanoparticles: preparation, functionalization and applications in biochemistry and immunochemistry. Russ Chem Rev 76:181–191
Dykman LA, Khlebtsov NG (2011) Gold nanoparticles in biology and medicine: recent advances and prospects. Acta Nat 3:34–55

Dykman L, Khlebtsov N (2012) Gold nanoparticles in biomedical applications: recent advances and perspectives. Chem Soc Rev 41:2256–2282

El-Sayed MA (2001) Some interesting properties of metals confined in time and nanometer space of different shapes. Acc Chem Res 34:257–264

Erik CD, Alaaldin MA, Xiaohua H, Catherine JM, Mostafa AE (2012) The golden age: gold nanoparticles for biomedicine. Chem Soc Rev 41:2740–2779

Farokhzad OC, Langer R (2009) Impact of nanotechnology on drug delivery. ACS Nano 3:16–20

Galla NR, Dubasi GR (2010) Chemical and functional characterization of gum karaya (*Sterculia urens L*) seed meal. Food Hydrocoll 24:479–485

Ghosh SK, Pal T (2007) Interparticle coupling effect on the surface plasmon resonance of gold nanoparticles: from theory to applications. Chem Rev 107:4797–4862

Huang X, El-sayed MA (2010) Gold nanoparticles: optical properties and implementations in cancer diagnosis and photothermal therapy. J Adv Res 1:13–28

Huang I, Li Q, Sun D, Lu Y, Su Y, Yang X, Wang H, Wang Y, Shao W, He N, Hong J, Chen C (2007a) Biosynthesis of silver and gold nanoparticles by novel sundried *Cinnamomum camphora* leaf. Nanotechnology 18:105104–105114

Huang CC, Yang Z, Lee KH, Chang HT (2007b) Synthesis of highly fluorescent gold nanoparticles for sensing mercury(II). Angew Chem Int Ed 46:6824–6828

Husen A (2017) Gold nanoparticles from plant system: synthesis, characterization and their application. In: Ghorbanpourn M, Manika K, Varma A (eds) Nanoscience and plant–soil systems, vol 48. Springer, Cham, pp 455–479

Husen A, Siddiqi KS (2014a) Carbon and fullerene nanomaterials in plant system. J Nanobiotechnol 12:16

Husen A, Siddiqi KS (2014b) Phytosynthesis of nanoparticles: concept, controversy and application. Nano Res Lett 9:229

Husen A, Siddiqi KS (2014c) Plants and microbes assisted selenium nanoparticles: characterization and application. J Nanobiotechnol 12:28

Ibrahim NA, Abo-Shosha MH, Allam EA, El-Zairy EM (2010) New thickening agents based on tamarind seed gum and karaya gum polysaccharides. Carbohydr Polym 81:402–408

Islam NU, Amin R, Shahid M, Amin M, Zaib S, Iqbal J (2017) A multi-target therapeutic potential of *Prunus domestica* gum stabilized nanoparticles exhibited prospective anti-inflammatory and analgesic properties. BMC Complement Altern Med 17:276–293

Jie H, Yan L, Rong G (2009) Facile synthesis of highly stable gold nanoparticles and their unexpected excellent catalytic activity for suzuki−miyaura cross-coupling reaction in water. J Am Chem Soc 131:2060–2061

Joshita D, Sutriyo PP, Anung P (2014) Antioxidant activity of gold nanoparticles using gum arabic as a stabilizing agent. Int J Pharm Pharm Sci 6:462–465

Kattumuri V, Katti K, Bhaskaran S, Boote EJ, Casteel SW, Fent GM, Robertson DJ, Chandrasekhar M, Kannan R, Katti KV (2007) Gum arabic as a phytochemical construct for the stabilization of gold nanoparticles: *in vivo* pharmacokinetics and X-ray-contrast-imaging studies. Small 3:333–341

Kora AJ, Arunachalam J (2012) Green fabrication of silver nanoparticles by gum tragacanth (*Astragalus gummifer*): a dual functional reductant and stabilizer. J Nanomater 2012:869765

Kora AJ, Sashidhar RB, Arunachalam J (2012) Aqueous extract of gum olibanum (*Boswellia serrata*): a reductant and stabilizer for the biosynthesis of antibacterial silver nanoparticles. Process Biochem 47:1516–1520

Kumar A, Ahuja M (2012) Carboxymethyl gum kondagogu: synthesis, characterization and evaluation as mucoadhesive polymer. Carbohydr Polym 90:637–643

Liu CP, Lin FS, Chien CT, Tseng SY, Luo CW, Chen CH, Chen JK, Tseng FG, Hwu Y, Lo LW, Yang CS, Lin SY (2013) In-situ formation and assembly of gold nanoparticles by gum arabic as efficient photothermal agent for killing cancer cells. Macromol Biosci 13:1314–1320

Llevot A, Astruc D (2012) Applications of vectorized gold nanoparticles to the diagnosis and therapy of cancer. Chem Soc Rev 41:242–257

Madhusudhan A, Reddy GB, Venkatesham M, Veerabhadram G, Kumar DA, Sumathi N, Ming YY, Anren H, Surya SS (2014) Efficient pH dependent drug delivery to target cancer cells by gold nanoparticles capped with carboxymethyl chitosan. Int J Mol Sci 15:8216–8234

Maity S, Sa B (2014) Ca-carboxymethyl xanthan gum mini-matrices: swelling, erosion and their impact on drug release mechanism. Int J Biol Macromol 68:78–85

Mayer KM, Hafner JH (2011) Localized surface plasmon resonance sensors. Chem Rev 111:3828–3857

Mirhosseini H, Amid BT (2012) A review study on chemical composition and molecular structure of newly plant gum exudates and seed gums. Food Res Int 46:387–398

Mirkin CA (2005) The beginning of a *small* revolution. Small 1:14–16

Muddineti OS, Kumari P, Ajjarapu S, Lakhani PM, Bahl R, Ghosh B, Biswas S (2016) Xanthan gum stabilized PEGylated gold nanoparticles for improved delivery of curcumin in cancer. Nanotechnology 27(32):325101–325112

Ojha AK, Maiti D, Chandra K, Mondal S, Das Sadhan K, Roy D, Ghosh K, Islam SS (2008) Structural assignment of a heteropolysaccharide isolated from the gum of *Cochlospermum religiosum* (Katira gum). Carbohydr Res 19:1222–1231

Padil VV, Černík M (2015) Poly (vinyl alcohol)/gum karaya electrospun plasma treated membrane for the removal of nanoparticles (Au, Ag, Pt, CuO and Fe_3O_4) from aqueous solutions. J Hazard Mater 287:102–110

Pandey S, Goswami GK, Nanda KK (2013) Green synthesis of polysaccharide/gold nanoparticle nanocomposite: an efficient ammonia sensor. Carbohydr Polym 94:229–234

Pissuwan D, Niidome T, Cortie MB (2011) The forthcoming applications of gold nanoparticles in drug and gene delivery systems. J Control Release 5:65–71

Pooja D, Panyaram S, Kulhari H, Rachamalla SS, Sistla R (2014) Xanthan gum stabilized gold nanoparticles: characterization, biocompatibility, stability and cytotoxicity. Carbohydr Polym 110:1–9

Pooja D, Panyaram S, Kulhari H, Reddy B, Rachamalla SS, Sistla R (2015) Natural polysaccharide functionalized gold nanoparticles as biocompatible drug delivery carrier. Int J Biol Macromol 80:48–56

Prajapati VD, Jani GK, Moradiya NG, Randeria NP (2013a) Pharmaceutical applications of various natural gums, mucilages and their modified forms. Carbohydr Polym 92:1685–1699

Prajapati VD, Jani GK, Moradiya NG, Randeria NP, Nagar BJ (2013b) Locust bean gum: a versatile biopolymer. Carbohydr Polym 94:814–821

Punuri JB, Sharma P, Sibyala S, Tamuli R, Bora U (2012) *Piper betle*-mediated green synthesis of biocompatible gold nanoparticles. Int Nano Lett 2:18–27

Rana V, Rai P, Tiwary AK, Singh RS, Kennedy JF, Knill CJ (2011) Modified gums: approaches and applications in drug delivery. Carbohydr Polym 83:1031–1047

Rao K, Imran M, Jabri T, Ali I, Perveen S, Shafiullah AS, Shah MR (2017) Gum tragacanth stabilized green gold nanoparticles as cargos for naringin loading: a morphological investigation through AFM. Carbohydr Polym 15:243–252

Rivas L, Sanchez-Cortes S, Garcia-Ramos JV, Morcillo G (2001) Growth of silver colloidal particles obtained by citrate reduction to increase the raman enhancement factor. Langmuir 17:574–577

Saha K, Agasti SS, Kim C, Li X, Rotello VM (2012) Gold nanoparticles in chemical and biological sensing. Chem Rev 112:2739–2779

Saikat M, Ipsita KS, Syed SI (2012) Green synthesis of gold nanoparticles using gum polysaccharide of *Cochlospermum religiosum* (katira gum) and study of catalytic activity. Phys E 45:130–134

Sánchez MP, Boulaiz H, Ortega-Vinuesa JL, Peula-García JM, Aránega A (2012) Novel drug delivery system based on docetaxel-loaded nanocapsules as a therapeutic strategy against breast cancer cells. Int J Mol Sci 13:4906–4919

Sankar R, Rahman PKSM, Varunkumar K, Anusha C, Kalaiarasia A, Subramanian K, Shivashangaric KS, Ravikumara V (2017) Facile synthesis of *Curcuma longa* tuber powder engineered metal nanoparticles for bioimaging applications. J Mol Struct 1129:8–16

Selvi SK, Mahesh J, Sashidhar RB (2017) Anti-proliferative activity of gum kondagogu (*Cochlospermum gossypium*)-gold nanoparticle constructs on B16F10 melanoma cells: an *in vitro* model. Bioact Carbohydrates Diet Fibre 11:38–47

Sermon PA, Bond GC, Wells PB (1979) Hydrogenation of alkenes over supported gold. J Chem Soc Farady Trans 1(75):385–394

Siddiqi KS, Husen A (2016a) Fabrication of metal nanoparticles from fungi and metal salts: scope and application. Nano Res Lett 11:98

Siddiqi KS, Husen A (2016b) Fabrication of metal and metal oxide nanoparticles by algae and their toxic effects. Nano Res Lett 11:363

Siddiqi KS, Husen A (2016c) Engineered gold nanoparticles and plant adaptation potential. Nano Res Lett 11:400

Siddiqi KS, Husen A (2016d) Green synthesis, characterization and uses of palladium/platinum nanoparticles. Nano Res Lett 11:482

Siddiqi KS, Husen A (2017a) Recent advances in plant-mediated engineered gold nanoparticles and their application in biological system. J Trace Elements Med Biol 40:10–23

Siddiqi KS, Husen A (2017b) Plant response to engineered metal oxide nanoparticles. Nano Res Lett 12:92

Siddiqi KS, Rahman A, Tajuddin HA (2016) Biogenic fabrication of iron/iron oxide nanoparticles and their application. Nano Res Lett 11:498

Siddiqi KS, Husen A, Rao RAK (2018a) A review on biosynthesis of silver nanoparticles and their biocidal properties. J Nanobiotechnol 16:14

Siddiqi KS, Rahman A, Tajuddin HA (2018b) Properties of zinc oxide nanoparticles and their activity against microbes. Nano Res Lett 13:141

Siddiqi KS, Husen A, Sohrab SS, Osman M (2018c) Recent status of nanomaterials fabrication and their potential applications in neurological disease management. Nano Res Lett 13:231

Subramanian SB, Bezawada SR, Dhamodharan R (2016) Green, selective, seedless and one-pot synthesis of triangular Au nanoplates of controlled size using bael gum and mechanistic study. ACS Sustain Chem Eng 4:3830–3839

Tagad CK, Rajdeo KS, Kulkarni A, More P, Aiyer RC, Sabharwal S (2014) Green synthesis of polysaccharide stabilized gold nanoparticles: chemo catalytic and room temperature operable vapor sensing application. RSC Adv 4:24014–24019

Thanaa IS, Rasha SSE, Suzan AAE (2015) Green synthesis of gold nanoparticles using cumin seeds and gum arabic: studying their photothermal efficiency. Nanosci Nanotechnol 5:89–96

Venkatpurwar V, Shiras A, Pokharkar V (2011) Porphyran capped gold nanoparticles as a novel carrier for delivery of anticancer drug: *in vitro* cytotoxicity study. Int J Pharm 409:314–320

Vieira S, Vial S, Maia FR, Carvahlo M, Reis RL, Granja PL, Oliveira M (2015) Gellan gum-coated gold nanorods: an intracellular nanosystem for bone tissue engineering. RSC Adv 5:77996–78005

Vinod VT, Saravanan P, Sreedhar B, Devi DK, Sashidhar RB (2011) A facile synthesis and characterization of Ag, Au and Pt nanoparticles using a natural hydrocolloid gum kondagogu (*Cochlospermum gossypium*). Colloids Surf B Biointerfaces 3:291–298

Wu CC, Chen DH (2010) Facile green synthesis of gold nanoparticles with gum arabic as a stabilizing agent and reducing agent. Gold Bull 43:234–240

Wu YL, Li YN, Liu P, Gardner S, Ong BS (2006) Studies of gold nanoparticles as precursors to printed conductive features for thin film transistors. Chem Mater 18:4627–4632

Zhang Z, Wu Y (2010) Investigation of the $NaBH_4$-induced aggregation of Au nanoparticles. Langmuir 26:9214–9223

Zharov VP, Kim JW, Curiel DT, Everts M (2005) Self-assembling nanoclusters in living systems: application for integrated photothermal nanodiagnostics and nanotherapy. Nanomed Nanotechnol Biol Med 1:326–345